Polymer 50 (2009) 2290–2293

Contents lists available at ScienceDirect

Polymer

journal homepage: www.elsevier.com/locate/polymer

Synthesis of core–shell structured PS/Fe_3O_4 microbeads and their magnetorheology

Fei Fei Fang, Ji Hye Kim, Hyoung Jin Choi*

Department of Polymer Science and Engineering, Inha University, Incheon 402-751, Republic of Korea

ARTICLE INFO

Article history:
Received 3 December 2008
Received in revised form
22 February 2009
Accepted 7 March 2009
Available online 25 March 2009

Keywords:
Magnetorheological fluid
Microbead
Magnetite

ABSTRACT

Most magnetic materials possess serious sedimentation problem due to their large density when they are adopted as magnetorheological (MR) materials. In this communication, we fabricated novel core–shell structured polystyrene(PS)/Fe_3O_4 microbeads via a facile method. Porous morphology of the PS obtained by etching silica particles and the loaded Fe_3O_4 was observed via both SEM and TEM images. XRD pattern confirms crystalline structure of the synthesized iron species. VSM data indicate the change in saturation magnetization before and after introducing organic PS core. Finally, MR performances of the PS/Fe_3O_4 based MR fluid were investigated via a rotational rheometer and sedimentation stability was found to be improved with a decreased density of the synthesized microbeads.

1. Introduction

Magnetorheological (MR) fluids which are colloidal suspensions of soft ferro-/ferri-magnetic particles in nonmagnetic medium are able to exhibit rapid state change between liquid-like and solid-like state with an aid of external magnetic field [1–7]. During this process, their rheological properties (yield stress, apparent viscosity, storage modulus, etc.) are being rapidly altered. Therefore, MR fluids, along with their electrically analogous electrorheological (ER) fluids [8–10] attract considerable attentions in widespread application of designing damper, torque transducer or polishing devices [11,12]. So far, the most popular MR materials are carbonyl iron (CI) particles (CD grade, BASF Germany, average particle size: 4.25 μm, density: 7.91 g/cm^3) due to their high saturation magnetization and proper particle size [13–15]. However, the large density of CI particles which causes serious sedimentation problem has limited their further engineering application. Thus, plenty of efforts (introducing additives or polymer coating technology) have been paid on preventing CI particles' contact and decreasing CI particles' density to improve the sedimentation stability [16–21]. Compared with the complicated process of modifying CI particles, another magnetic species, magnetite (Fe_3O_4) particles with much lower density (4.32 g/cm^3) but enough good magnetic behavior comes to front [22,23]. In this work, aiming to reduce the density mismatch between Fe_3O_4 and medium oil (0.96 g/cm^3) as well as the aggregation problem of nano-scaled Fe_3O_4 particles, polystyrene (PS) microspheres wrapped by amorphous silica were initially synthesized via facile suspension polymerization, then etching process for the silica particles was undergone in HF bath to form microporous PS particles, finally, Fe_3O_4 particles were loaded on the surface of microporous PS particles via a typical conventional oxidative reaction. The morphology of product in each step was observed via SEM/TEM view. In addition, whether genuine Fe_3O_4 rather than Fe_2O_3 or other iron species were synthesized was confirmed via XRD pattern. MR performances of the synthesized PS/Fe_3O_4 particle based MR fluid were investigated as a function of magnetic field strength. Finally, the sedimentation stability was also checked by testing the density of PS/Fe_3O_4 particles.

2. Experimental part

First, micron-sized PS/silica particle was synthesized via suspension polymerization in the presence of stabilizer (polyvinyl alcohol/PVA). Commercial silica particles were dispersed in styrene monomer by using ultrasonication. This prepared styrene/silica mixture was added in PVA solution with vigorous stirring. In this process, solid silica particles in the mixture moved out to the monomer droplet and were presented in the interface of monomer and aqueous solution due to hydrophilicity of the silica particles. Then, the nonionic oil-soluble initiator, 2,2′-azobisisobutyronitrile (AIBN) was added into the reactor to initiate polymerization. The reaction was maintained at 60 °C for 12 h.

* Corresponding author. Tel.: +82 32 860 8777; fax: +82 32 860 7486.
E-mail address: hjchoi@inha.ac.kr (H.J. Choi).

0032-3861/$ – see front matter © 2009 Elsevier Ltd. All rights reserved.
doi:10.1016/j.polymer.2009.03.023

To obtain the core material of porous PS particles, silica deposited on the surface of PS/silica particles was removed by etching in 10 M hydrofluoric acid bath. Then, the obtained microporous PS particles were washed by di-water via a centrifuge to remove the impurity, and then added in the aqueous SDS (sodium dodecylsulfate) solution to wait for the synthesis of Fe_3O_4. In order to deposit Fe_3O_4 particles on the surface of microporous PS, $FeCl_2$ and $FeCl_3$ aqueous solution (1:2 mol ratio) were added subsequently [24–26]. After that, the mixture was heated to 80 °C and added with 5 M NaOH solution slowly. After 4 h, the product was washed with excess distilled water and methanol, and then dried at 65 °C in vacuum oven for 2 days. The chemical equation of forming magnetite particles is:

$$Fe^{2+} + 2Fe^{3+} + 8OH^- \rightarrow Fe_3O_4 + 4H_2O$$

Pure Fe_3O_4 particles used in this work were also synthesized following the same way only without using porous PS spheres.

Morphology of PS/silica, microporous PS and PS/Fe_3O_4 was observed by both scanning electron microscope (SEM, S-4300, Hitachi Japan) and transmission electron microscope (TEM, Philips CM200). The sampling for TEM view was done by an initial moulding of particles in epoxy, following nano-scaled cutting by using an ultramicrotome (UMT) as well as a final dropping on a copper grid. Furthermore, XRD spectra were obtained via a Rigaku DMAX 2500 (Cu Kα, $\lambda = 1.54$ Å) diffractometer to confirm the successfully synthesized Fe_3O_4.

The MR fluid was prepared by dispersing PS/Fe_3O_4 particles in silicone oil (kinematic viscosity: 50 cS, density: 0.96 g/ml) with 11 vol% via a sonicator for 1 h to obtain good dispersion. Then, a rotational rheometer (Physica MC 300, Stuttgart) equipped with a magnetic field generator was used to perform MR characterization at room temperature. A parallel-plate measuring system with a diameter of 20 mm was used at a gap of 1 mm. Finally, density of synthesized magnetic PS/Fe_3O_4 particles was examined by using pyconometer.

3. Results and discussion

Morphology of the PS particles before and after silica etching is indicated in Fig. 1. Before being etched with HF as shown in Fig. 1(a), spherical PS/silica particles with an average diameter of about 50 μm exhibit considerably rough surface due to the deposit of silica particles. After etching in HF bath (Fig. 1(b)), silica particles disappeared completely and left plenty of micropores randomly spread over the surface of PS particles. Simultaneously, the surface of PS particles changes to be much smoother than the surface before etching.

On the other hand, Fig. 2(a) shows the morphology of PS particles after loading Fe_3O_4 particles. The inset picture is a magnified view for one PS/Fe_3O_4 particle. Compared with the smooth surface of PS particles with a microporous structure, the Fe_3O_4 loaded PS spheres exhibit very rough appearance, in which all of micropores are chocked up with Fe_3O_4 particles, thus a thick shell of Fe_3O_4 onto the core of PS microspheres can be assumed. Although a perfect spherical profile of core–shell structured PS/

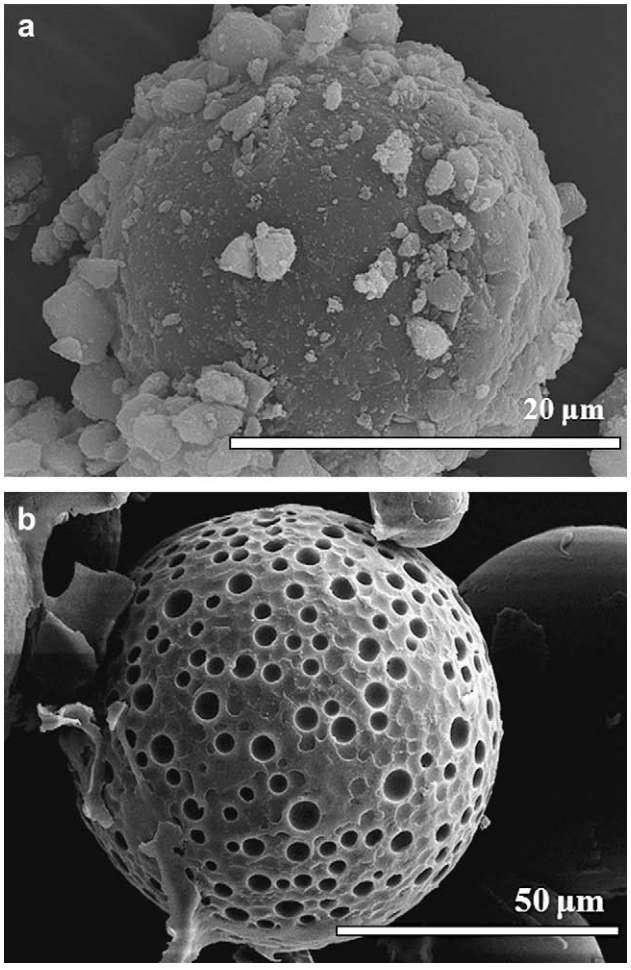

Fig. 1. SEM images of microporous PS particles before (a) and after (b) HF etching.

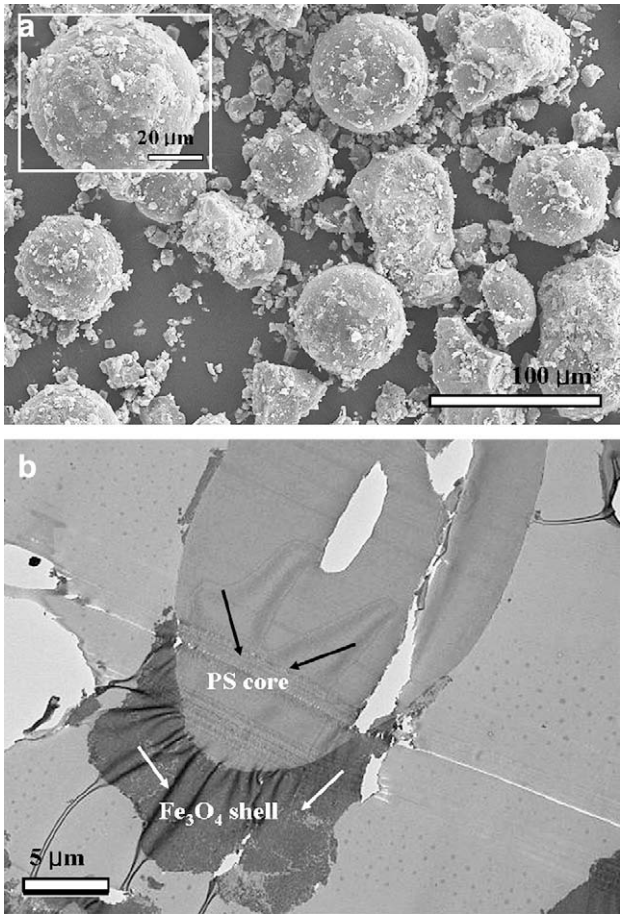

Fig. 2. SEM (a) and TEM (b) images of Fe_3O_4 coated microporous PS particles.

Fe_3O_4 particles has been expected, some irregular coated composite particles are still visible making the coating layer uneven and nonuniform.

Furthermore, in order to observe the coating characteristics of Fe_3O_4 nanoparticles, a cross-section view was observed via TEM by cutting the mold of particles in epoxy into nano-scaled sheets. From TEM image shown in Fig. 2(b), the grey part in the center represents the organic PS core as marked by black arrow head, while the outside black part is considered to be aggregation of inorganic Fe_3O_4 nanoparticles as pointed with a white arrow head. Additionally, besides the region which was covered by Fe_3O_4 aggregation, some naked parts were also visible. Therefore, we can conclude that the coating layer composed of Fe_3O_4 nanoparticles on the surface of microporous PS spheres is not uniform.

Whether the expected Fe_3O_4 particles rather than other iron species were synthesized was confirmed via XRD patterns. In order to compare the crystalline structure to define the iron species, XRD characterization of both commercial Fe_3O_4 particles purchased (Aldrich Chemical Company (USA)) and pure Fe_3O_4 particles which were fabricated in the same method with that of PS/Fe_3O_4 were also undertaken. In Fig. 3(a), the spectra of synthesized Fe_3O_4 and Fe_3O_4 coated PS spheres indicate similar characteristic peaks with commercial Fe_3O_4 particles at 2θ (Brag angle) value of 30.1, 35.5, 43.2, 53.5, 57.1, 62.6°, which corresponds to the typical peaks of

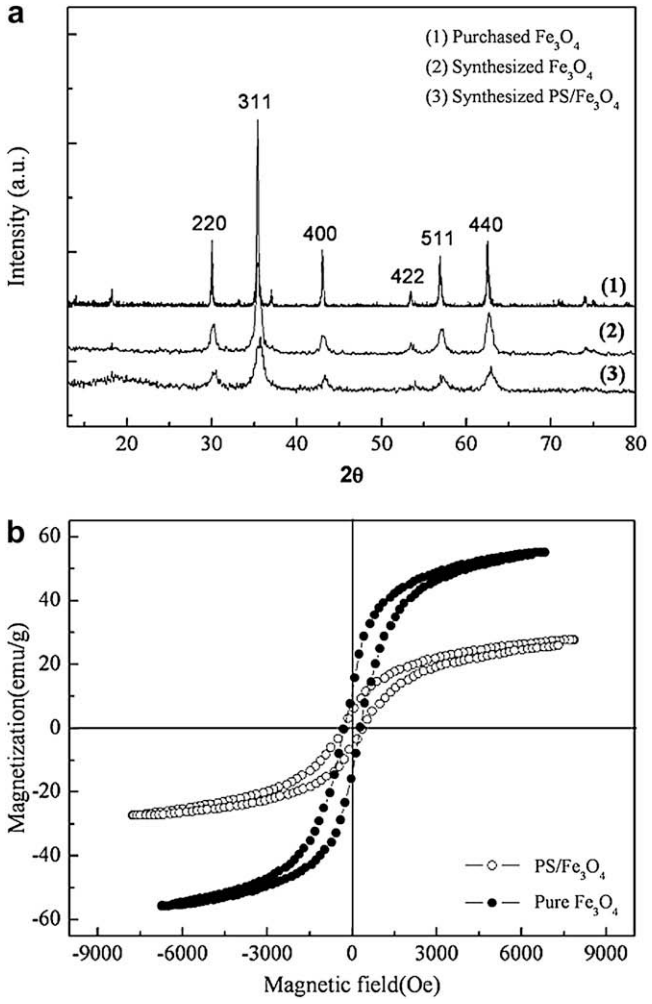

Fig. 3. (a) XRD pattern of purchased Fe_3O_4 (1), synthesized Fe_3O_4 (2) and PS/Fe_3O_4 particles (3), and (b) VSM data for pure Fe_3O_4 (closed symbol) and PS/Fe_3O_4 particles (open symbol).

Fe_3O_4 particles [27]. So, there is no doubt that Fe_3O_4 particles are synthesized successfully. Comparing purchased Fe_3O_4 with synthesized pure Fe_3O_4 particles, PS/Fe_3O_4 particles display a little amorphous peak at lower 2θ range ($2\theta < 20°$) as well as much decreased peak intensity at higher 2θ range (70°–80°). This is attributed to the introduction of organic PS core. In addition, the mean crystallite size of synthesized Fe_3O_4 nanoparticles can be calculated via Scherrer equation as follows [28]:

$$D = \frac{k\lambda}{\beta \cos\theta} \tag{1}$$

where λ is the wave-length of the incident X-rays (Cu Kα, $\lambda = 1.54$ Å), k is a unit cell geometry dependent constant whose value is typically between 0.85 and 0.99. D is the average diameter of the crystals, θ is the Bragg angle and β is the full width at half maximum (FWHM) of the diffraction peaks (in radian). Thereby, the mean crystallite size of Fe_3O_4 nanoparticles was calculated to be about 9 nm when k was assumed to be 0.89 related to the shape and index (hkl) of the crystals [29–31]. This result reveals that the Fe_3O_4 covered on the surface of PS cores was aggregated nano-scaled Fe_3O_4 nanoparticles with good crystal structure.

The magnetic hysteresis loops measured in a powder state for synthesized pure Fe_3O_4 and PS/Fe_3O_4 particles are represented in Fig. 3(b). The saturation magnetization for PS/Fe_3O_4 composite particles is about 27 emu/g, which is much lower than that of pure Fe_3O_4 (57 emu/g) due to the introduction of organic PS core. Thus, MR suspension based on PS/Fe_3O_4 particles will possess weak MR performances compared with that of pure Fe_3O_4 particles, because the saturation magnetization is a very crucial factor for superior MR effect. In addition, the intrinsic hysteresis behavior for Fe_3O_4 particles is well sustained in PS/Fe_3O_4 composite particles.

The MR characterization was performed via controlled shear rate (CSR) mode for the pure Fe_3O_4 and PS/Fe_3O_4 particle based MR fluid. The range of shear rate tested was from 0.01 to 200 s^{-1} via a log–log scale. Note that shearing MR fluids with too high shear rate may cause expelling the MR fluid between the disks. For each shear rate sweep, the measuring point's duration was set from an initial 10 s to a final 1 s via log–log scale. The resulting flow responses were examined as a function of magnetic field strength ranging from 0 to 343 kA/m as indicated in Fig. 4(a). Both the two systems represent similar Bingham behavior, in which a plateau behavior is observed at relatively low shear rate range and a nearly linear behavior at very high shear rate in a log–log plot [19,32,33]. As expected, the obtained shear stress has a strong dependence on the applied field strength, which is similar with the phenomenon observed for ER fluids [34]. This observation is attributed to the formed robust columns due to the strong dipole–dipole interaction among the adjacent magnetic particles. Based on shear stresses observed, we find that introducing polymeric core inevitably brings negative effect on the shear stress compared with pure Fe_3O_4 particles; however the typical MR behavior was reserved [18,35]. This result coincides with the VSM hysteresis loops regarding saturation magnetization.

Finally, we checked the sedimentation stability. By using organic microporous PS as a core, the density of PS/Fe_3O_4 particles is reduced to be 1.90 g/cm^3 which is nearly two-fifth of pristine Fe_3O_4 particles. Compared with pure Fe_3O_4 based MR fluid, the density mismatch between PS/Fe_3O_4 particles and continuous oil (0.96 g/cm^3) was obviously reduced. Thus, the sedimentation stability may be improved. Fig. 4(b) indicates the recorded sedimentation ratio as a function of time. The inset graph is a magnified view for the initial 5 h. It is obvious that PS/Fe_3O_4 suspension exhibits high sedimentation stability than that of pure Fe_3O_4 suspension in the same testing time duration. Pure Fe_3O_4 suspension settles down rapidly

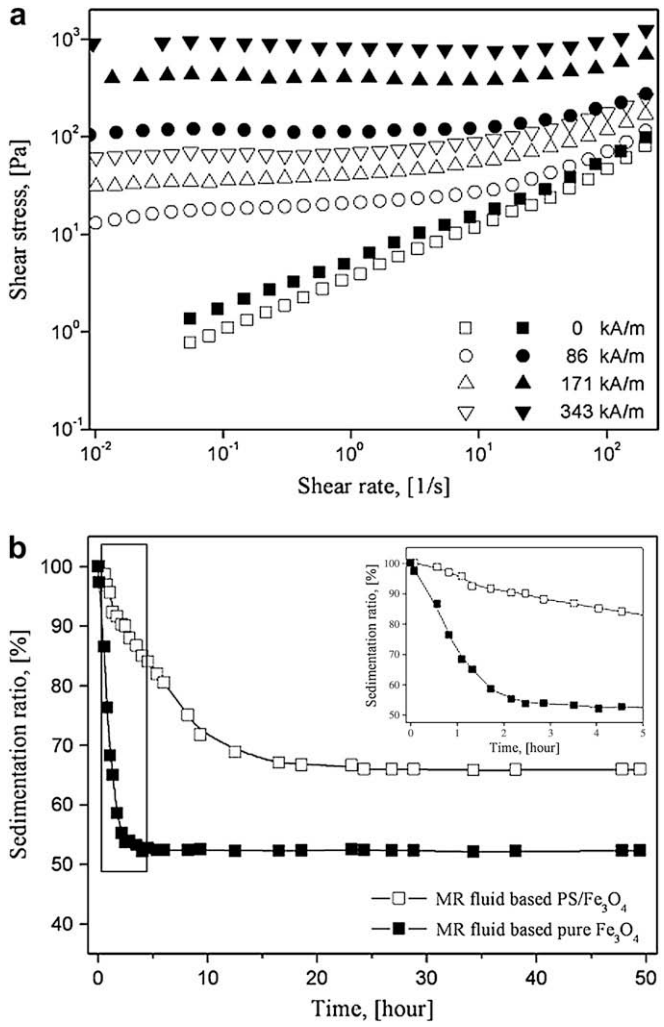

Fig. 4. Shear stress curves (a) and sedimentation ratio (b) of pure Fe_3O_4 (closed symbol) and PS/Fe_3O_4 spheres (open symbol) based MR fluid.

within the initial 2 h, while the PS/Fe_3O_4 suspension indicates nearly stable dispersion. Thus, loading Fe_3O_4 nanoparticles on the surface of porous PS spheres can improve the sedimentation problem due to apparently reduced mismatch in density. Polymer coating technology also gives the similar performance in reducing sedimentation rate [19,33–36].

4. Conclusion

In this work, novel PS/Fe_3O_4 particles with microporous PS as a core material and Fe_3O_4 as a shell material were prepared to improve sedimentation stability for the MR fluid. Microporous structure of the PS spheres along with the loaded Fe_3O_4 particles on the surface was confirmed via SEM/TEM images. XRD pattern verifies the accurate crystalline structure of synthesized Fe_3O_4 particles. VSM graph indicates that introducing hollow PS spheres makes saturation magnetization decease from 57 emu/g for pure Fe_3O_4 to 27 emu/g for PS/Fe_3O_4 composite particles. Although MR characterization exhibits lower shear stress value compared with pure Fe_3O_4 based MR fluid, the typical MR behavior was well preserved. Further effort should be paid on fabricating PS/Fe_3O_4 composite particles with much smaller PS core and thicker Fe_3O_4 layer which is considered to be a crucial role in presenting superior MR properties. At last, sedimentation rate was recorded to get much improved due to the decreased density mismatch between PS/Fe_3O_4 composite particles (1.90 g/cm^3) and medium oil (0.96 g/cm^3).

Acknowledgement

This research was supported by a grant from the Fundamental R&D Program for Core Technology of Materials funded by the Ministry of Knowledge Economy, Korea (2008).

References

[1] Winslow WM. J Appl Phys 1949;20:1137–40.
[2] Phule PP. Smart Mater Bull 2001 2001:7–10.
[3] Bossis G, Volkova O, Lacis S, Meunier A. In: Odenbach S, editor. Ferrofluids, magnetorheology: fluids, structure and rheology. Berlin: Springer; 2002.
[4] Bica I, Choi HJ. Int J Mod Phys B 2008;22:5041–64.
[5] Viota JL, de Vicente J, Duran JDG, Delgado AV. J Colloid Interface Sci 2005;284:527–41.
[6] Bombard AJF, Knobel M, Akantara MR. Int J Mod Phys B 2007;21:4858–67.
[7] Trendler AM, Bose H. Int J Mod Phys B 2007;21:4967–73.
[8] Choi HJ, Jhon MS. Soft Matter 2009, doi:10.1039/B818368F.
[9] Fang FF, Choi HJ, Joo J. J Nanosci Nanotechnol 2008;8:1559–81.
[10] Yin J, Zhao X, Xia X, Xiang L, Qiao Y. Polymer 2008;49:4413–9.
[11] Bica I. J Ind Eng Chem 2007;13:693–711.
[12] Bossis G, Khuzir P, Lacis S, Volkova O. J Magn Magn Mater 2003;258–259:456–8.
[13] Rankin PJ, Horvath AT, Klingenberg DJ. Rheol Acta 1999;38:471–7.
[14] Tang X, Zhang X, Tao R, Rong Y. J Appl Phys 2000;87:2634–8.
[15] Ulicny JC, Golden MA, Namuduri CS, Klingenberg DJ. J Rheol 2005;49:87–104.
[16] de Vicente J, López-López MT, Duran JDG, Bossis G. J Colloid Interface Sci 2005;282:193–201.
[17] Fang FF, Jang IB, Choi HJ. Diamond Relat Mater 2007;16:1167–9.
[18] Lim ST, Choi HJ, Jhon MS. IEEE Trans Magn 2005;41:3745–7.
[19] Cho MS, Lim ST, Jang IB, Choi HJ, Jhon MS. IEEE Trans Magn 2004;40:3036–8.
[20] Fang FF, Choi HJ. Phys Stat Sol (a) 2007;204:4190–3.
[21] Fang FF, Choi HJ. J Appl Phys 2008;103:07A301.
[22] Samouhos S, McKinley G. J Fluid Eng-T ASME 2007;129:429–37.
[23] Kanno H, Shimada K, Ogawa J, Inoue N. Int J Appl Electrom 2007;25:109–12.
[24] Kin DK, Zhang Y, Voit W, Rao KV, Muhammed M. J Magn Magn Mater 2001;225:30–6.
[25] Wu KT, Kuo PC, Yao YD, Tsai EH. IEEE Trans Magn 2001;37:2651–3.
[26] Chen A, Wang H, Zhao B, Li X. Synth Met 2003;139:411–5.
[27] Klong HP, Alexander LE. X-ray diffraction procedure for crystalline and amorphous materials. New York: Wiley; 1954.
[28] Vereda F, de Vicente J, del Puerto Morales M, Rull F, Hidalgo-Álvarez R. J Phys Chem C 2008;112:5843–9.
[29] Wan M, Zhou W, Li J. Synth Met 1996;78:27–31.
[30] Deng J, Peng Y, He C, Long X, Li P, Chan ASC. Polym Int 2003;52:1182–7.
[31] Qiu G, Wang Q, Nie M. Macromol Mater Eng 2006;291:68–74.
[32] Park JH, Chin BD, Park OO. J Colloid Interface Sci 2001;240:349–54.
[33] Jang IB, Kim HB, Lee JY, You JL, Choi HJ, Jhon MS. J Appl Phys 2005;97:10Q912.
[34] Choi HJ, Kim TW, Cho MS, Kim SG, Jhon MS. Eur Polym J 1997;33:699–703.
[35] Kim JH, Fang FF, Choi HJ, Seo Y. Mater Lett 2008;62:2897–9.
[36] Lee MA, Fang FF, Choi HJ. Phys Stat Sol (a) 2007;204:4186–9.